EVALUATION OF PRINCIPAL COMPONENTS FOR LAND COVER DISCRIMINATION USING OBJECT-BASED CLASSIFICATION

Nyamjargal Erdenebaatar[13], Enkhmanlai Amarsaikhan[2], Amarsaikhan Damdinsuren[1], Sodnom Enkhtuya[3]
[1]Instiutute of Geography and Geoecology, Mongolian Academy of Sciences
[2]Oyuny tsomorlig impex LLC, Ulaanbaatar, Mongolia
[3]National University of Technology, Ulaanbaatar, Mongolia
Email: nyamjargale@mas.ac.mn

KEY WORDS: Feature extraction, object-based classification, principal component analysis (PCA)

ABSTRACT: In remote sensing (RS) applications, a PCA is generally used for reduction of data dimensionality, and fusion of different datasets. Many studies have used the PCA for these purposes, but the most common application is a reliable feature extraction before conducting any classification procedures. The aim of this study is to evaluate the features obtained from the PCA for a mixed land cover classification. As data sources, dual polarization Sentinel-1 synthetic aperture radar (SAR) image and Sentinel-2 multispectral bands of the Erdenet area, northern Mongolia are selected. For the feature extraction, the PCA is applied to the fused microwave and optical datasets. As a method for the land cover classification, an object-based classification technique is selected, and four different combinations of the principal component (PC)s such as PC123, PC236, PC2345, and PC123456 are evaluated. Of the selected PC combinations, the highest overall classification accuracy is achieved in the PC236 combination. Overall, the research indicates that although the majority of the data information is contained in PC1, the PCs that contain insignificant amount of variance can still include some useful information for land cover discrimination.

1. INTRODUCTION

Data acquisitions from multi-sensor RS have different inherent advantages and disadvantages for land use/land cover studies and other image-based thematic analyses. For example, SAR imagery acquired at different radar frequencies measures physical properties of the observed scene and can be received at all weather and at daylight/night conditions, while multispectral imagery acquired at different portions of the optical range measures spectral characteristics of the Earth's surface objects and needs daylight without cloud coverage for analysis. Multispectral data is much easier to interpret visually, whereas microwave data contains not only amplitude, but also phase information, which enables other advanced analyses, including high-precision measurement of three-dimensional topography. However, in most cases SAR datasets suffer from the presence of speckles (Datta, 2021), and it is not easy task to completely remove them from the analyzed images. Considering the advantages of both sources, a combined use of these datasets should have a great number of applications in many different fields (Amarsaikhan and Ganchuluun, 2015).

One of the most recognizable methods to combine multisource datasets is image fusion. The image fusion refers to a process that integrates different images from a variety of sources to obtain more information, considering a minimum loss or distortion of the original dataset. In other words, the image fusion is the integration or combination of different digital images in order to create a new image and obtain more information than can be derived separately from any of them (Amarsaikhan and Ganchuluun, 2015). In the field of digital processing of RS datasets, this technique usually attempts to combine the images with different spectral, spatial, and temporal resolutions and increase detailed information in the hybrid product (Sritarapipat et al. 2014). Over the years, different fusion methods have been developed among the RS community for improving spectral and spatial resolutions of the existing sensor datasets (Fang et al. 2013; He and Yokoya, 2018). However, the PCA is still extensively used for the fusion of various datasets with different characteristics.

There are many examples of the PCA for successful fusion of optical and radar imageries. Amarsaikhan and Saandar (2011) used the PCA for fusion of multichannel ASTER and HH, HV, and VV polarization components of ALOS PALSAR1 to enhance spectral variations of urban land surface features, and apply the selected features for land cover mapping. Comber et al. (2016) and Haruna (2019) applied the PCA for combining Sentinel-1 and Sentinel-2 imageries in order to classify land cover types as well as to improve the classification accuracy. Quang et al. (2019) used the PCA along with some other techniques to fuse Landsat 8 and Sentinel-1 images in order to produce higher quality, fine resolution colour visualizations, and to reduce the effects of clouds and shadows in optical images. Neetu and Ray (2020) evaluated the performances of the PCA and some other combinations of data fusion techniques at pixel, feature, and decision level for crop classification using Sentinel-1 and Resourcesat-2 LISS III datasets.

The aim of this research is to evaluate the reliabilities of the selected features obtained from the PCA via a feature reduction process for a land cover classification in Erdenet area, northern part of Mongolia and to determine the best combination of the used PCs. For this purpose, an object-based classification has been applied and combined Sentinel-

1 microwave and Sentinel-2 multispectral images were used.

2. STUDY AREA AND DATA SOURCES

2.1 The study area

As a test site, Erdenet area of Orkhon province, northern Mongolia has been selected. The site is located at about 330km toward the northwest from the capital city of Ulaanbaatar (centered at: 49°01′ 40″ N 104°02′ 40″ E) (Figure 1). The area hosts the fourth largest copper mine in the world. Erdenet city currently has the highest per capita GDP in Mongolia, as a result of the operations of the Erdenet Mining Corporation's activities. The province itself is home to around 89,000 inhabitants and is one of only three provinces (not including the capital city) that experienced positive net migration over the past decade (https://www.toursmongolia.com/destinations/erdenet-city). The Area of Interest (AOI) was delimited considering the surrounding area of the city in order to classify different land cover types during the analysis. The study site has an area of 520 sq.km.

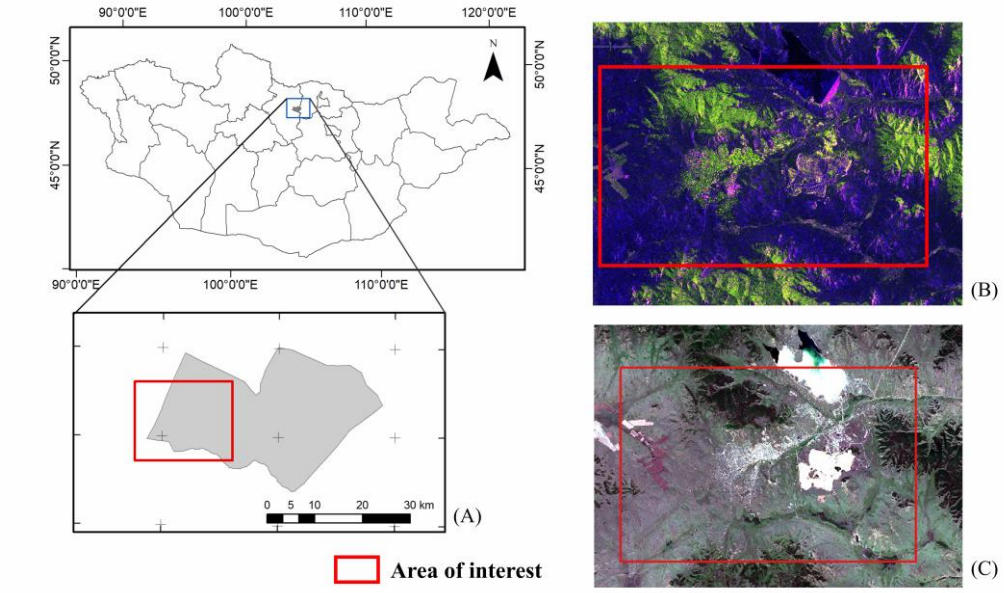

Figure 1. Location of study site in relation to Orkhon province (A);
Study site (red square) shown in Sentinel-1 (B), and Sentinel-2 (C) images.

2.1 Data description and data preprocessing

With the Copernicus program and its Sentinel satellites, a growing source of satellite RS data is publicly available at no charge. In our study, Sentinel-1B imagery acquired on 14 June 2021, and Sentinel-2B optical data dated on 9 June 2021, were used. Sentinel-1B data was recorded in interferometric wide swath mode with dual polarizations. Sentinel-2 has four bands with 10 m, six bands with 20 m, and three bands with 60 m spatial resolutions, respectively (Drusch et al. 2012; Wang & Atkinson, 2018). In the present study, multisepctral bands with a spatial resolution of 10 m, and shortwave-infrared bands with a spatial resolution of 20 m have been selected.

A standard generic workflow to preprocess Sentinel-1 GRD data includes a series of standard corrections, applying a precise orbit of acquisition, removing thermal noise, performing radiometric calibration, and applying range Doppler and terrain correction. The Sentinel Application Platform (SNAP) version 8.0 has been used for processing of Sentinel-1 data. For Sentinel-2 image, atmospheric correction and resampling at 10 m resolution using SNAP is required to ensure all bands have equal spatial resolution during image fusion.

3. METHODOLOGY

The processing chain that has been carried out for the land cover classification is illustrated in Figure 2. The processing steps of the combined multisource images are as follows:

- Preprocessing of the datasets;
- Merging preprocessed Sentinel-1B and Sentinel-2B images using the PCA;
- Classifying by the use of object-based method;

- Assessing the accuracies using overall accuracy and kappa coefficients.

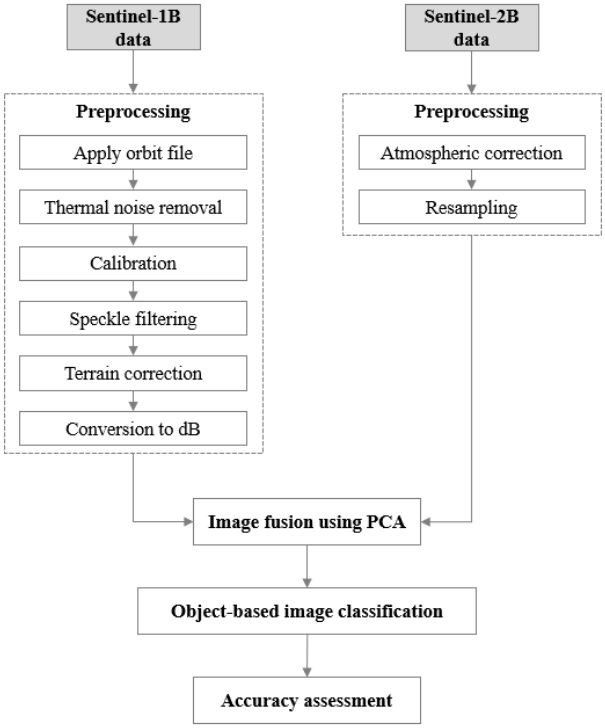

Figure 2. The analysis flowchart of multisource images.

3.1 The analysis using the PCA

In RS applications, after applying the PCA technique, the bands become more non-correlated and often more interpretable than the source data. When the PCA is performed, the axes of the spectral space are rotated, changing the coordinates of each pixel in spectral space. The new axes are parallel to the axes of the ellipse. The length and direction of the widest transect of the ellipse are calculated using a matrix algebra. The transect, which corresponds to the major axis of the ellipse, is called the first principal component of the data. The second principal component is the widest transect of the ellipse that is perpendicular to the first principal component. In n dimensions, there are n principal components. Each successive principal component is the widest transect of the ellipse that is orthogonal to the previous components in the n-dimensional space, and accounts for a decreasing amount of the variation in the data which is not already accounted for by previous principal components (Munkh-Erdene et al. 2021).

Mathematical and statistical concepts used to calculate the PCA are variance, covariance, eigenvalues, eigenvectors and linear transformations. It is applicable to dataset of any number of bands, and any three of the resulting components may be displayed as a color composite. PC image is generated as the sum of the products of eigenvectors and DN values for respective spectral bands at each pixel. Obviously, a larger numeric value of eigenvector (positive or negative) has a higher influence on the PC image. A low numeric value of eigenvector implies the particular band has relatively low significance for that PC axis (Ravi et al. 2013).

3.2 Object-based classification

Traditionally, pixel-based classification techniques have been extensively used for a thematic mapping of RS images (Amarsaikhan and Ganchuluun, 2015). The pixel-based methods analyze the spectral properties of every pixel within the selected image frame, without taking into account some important characteristics related to the pixel of interest (i.e. the information from surrounding pixels, which may help in correctly identifying the target pixel's class). With the growing availability of more datasets, other properties, including the spatial or contextual information could be effectively used to produce more accurate classification results, thus promoting development of an object-based technique (Nyamjargal et al. 2020).

In recent years, object-based methods have been successfully used for a land cover classification. The method is based on the information from a set of similar pixels called image objects. Image objects are groups of pixels that are similar to one another based on the spectral properties, size, shape, and texture, as well as context from a neighborhood surrounding the pixels. The object-based method uses a segmentation process and iterative learning

algorithm to achieve a semi-automatic classification procedure that demonstrates more accurate results than traditional pixel-based methods (Grenzdorffer, 2005; Liu and Xia, 2010; Weih & Riggan, 2012).

In our study, the training and test data are manually extracted and labeled from the high resolution images of Google Earth. Four classes have been selected to represent the land use/land cover classes of the selected study area, namely, forest, vegetation, water bodies, and other (mixed) class, and thirty signatures (polygons) were collected in each class. The final object-based classification has been performed by the use of eCognition Developer 9.0.

3.3 Accuracy assessment

Validation and accuracy assessments are important in the assessment of the performances of the selected PCs for land cover discrimination in the target area. The results of the object-based classifications have been evaluated in terms of the overall accuracy (OA) statistical index and kappa coefficients. The kappa coefficient is calculated from the error matrix and measures how the classification performs compared to the reference data.

4. RESULTS AND DISCUSSION

Initially, the fusion of multispectral Sentinel-2 bands with the polarization components of the Sentinel-1 microwave data has been conducted using the PCA. For the merging of the multisource datasets, SNAP 8.0 software was used. After the PCA, each of the components was visually inspected. The analysis of the PCs revealed that the first 6 components contained some useful information, and the rest included the noise of the entire dataset. Figure 3 illustrates the first six PCs, and Table 1 shows the results of the PCA.

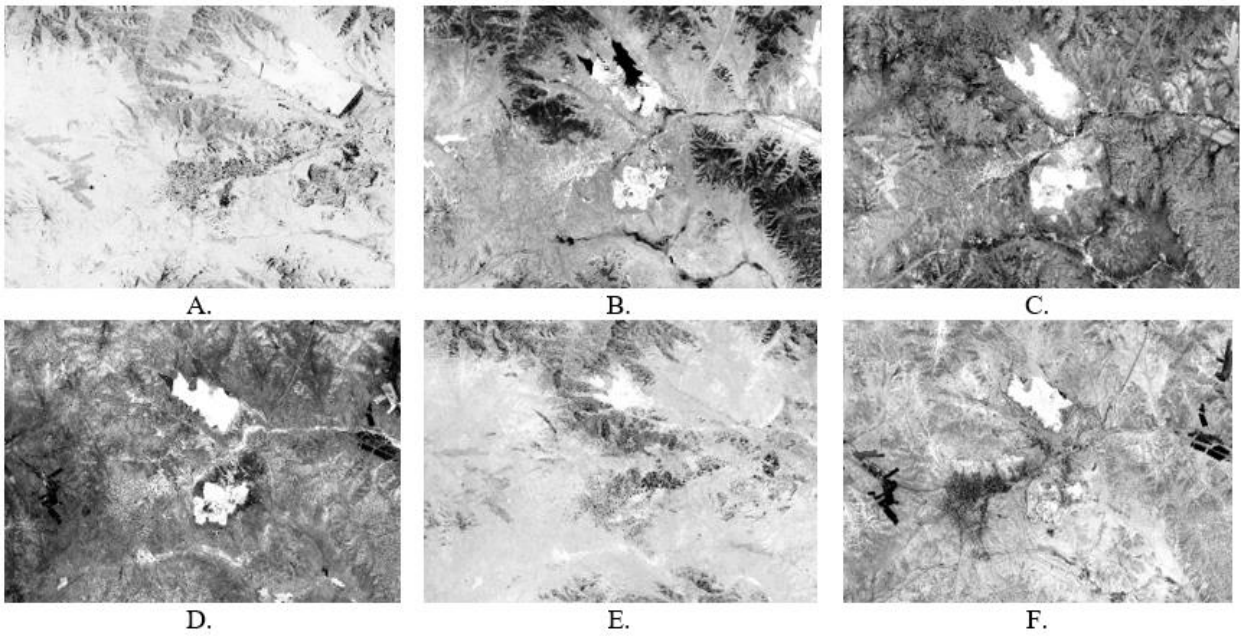

Figure 3. Comparison of the first six PCs.
(A) PC1, (B) PC2, (C) PC3, (D) PC4, (E) PC5, and (F) PC6.

As seen from the Figure 3a and Table 1, PC1 comprises moderate loadings of red-edge, NIR, and SWIR bands of the multispectral image. The SAR images have a very little influence on this component, whereas visible bands of the Sentinel-2 data have negligible effects. Although it contains 56.35% of the overall variance, visual inspection revealed that it contained less information related to the available classes. The PC2 includes moderate loadings of the visible red band and VV polarisation of microwave data. Other bands have little or negligible influences on this component. Even though it has 12.51% of the overall variance, visual inspection of the PC2 showed that it contained some useful information related to the existing land cover classes. In the PC3, SWIR band of the optical data has the highest loading, and VV polarisation includes the second highest influence. Other bands mainly have little negative influences. As seen from Table 1, PC4 is totally dominated by the variance (5.78%) of VH polarisation of the Sentinel-1 data. Here, other bands have almost no influences. The PC5 is dominated by the variance (5.19%) of the NIR, and other bands have insignificant influences. In the PC6, SWIR band has a high negative loading, while VV polarisation of SAR data has a high positive loading. Visual inspection of this PC indicated that it contained useful information about the classes though it contained only 4.22% of the overall variance.

Table 1. PC coefficients from the combined multisource images.

	PC1	PC2	PC3	PC4	PC5	PC6	PC7	PC8	PC9	PC10	PC11
Band 2	0.043	0.294	-0.355	-0.022	0.058	-0.256	0.586	-0.249	-0.260	0.490	-0.046
Band 3	0.082	0.295	-0.394	-0.025	0.103	-0.240	0.165	-0.177	0.334	-0.714	0.049
Band 4	0.076	0.448	-0.351	-0.013	0.030	0.160	-0.143	0.765	0.100	0.164	0.045
Band 5	0.165	0.313	-0.270	-0.014	-0.193	0.107	-0.609	-0.376	-0.478	-0.045	-0.102
Band 6	0.377	-0.120	-0.182	-0.012	0.303	0.093	-0.118	-0.247	0.492	0.319	0.542
Band 7	0.427	-0.205	-0.135	-0.010	-0.295	0.141	0.114	0.029	0.231	0.025	-0.764
Band 8a	0.472	-0.235	-0.101	-0.017	0.823	0.009	-0.156	-0.030	-0.047	0.078	-0.007
Band 11	0.465	-0.248	-0.003	-0.003	-0.267	0.029	0.303	0.276	-0.527	-0.318	0.322
Band 12	0.384	0.335	0.519	0.050	-0.082	-0.648	-0.151	0.093	0.070	0.073	0.051
SAR VV	0.219	0.492	0.433	0.043	0.116	0.625	0.268	-0.189	0.052	-0.071	0.030
SAR VH	-0.004	-0.021	-0.075	0.996	0.008	2.219	7.792	-0.004	-0.003	-0.002	-1.326
Eigenvalues	3380.0	750.5	483.1	346.7	311.3	253.3	193.5	136.1	82.3	59.1	3.4
Variance (%)	56.35	12.51	8.05	5.78	5.19	4.22	3.23	2.27	1.37	0.99	0.06

In the land cover discrimination, four different groups of the PC combinations such as PC123, PC236, PC2345, PC123456, have been defined. To extract land cover information, initially, we applied a multi-resolution segmentation followed by creation of a rule-base with different conditions to be fulfilled. In the rule-base, the entire image had to be divided into "water" and "forest" classes. After that unclassified image objects were classified into "vegetation" and "other" classes. A general diagram of the classification scheme is shown in Figure 4, and the results of the object-based method are shown in Figure 5.

As seen from the outputs of the classification, the forest was successfully classified in all PC images, whereas other-class was the most mixed class in all combinations. It is interesting to remark that although the fuzzy boundary between vegetation and forest classes has high statistical overlaps, the classes could still be separable on the selected PC combinations.

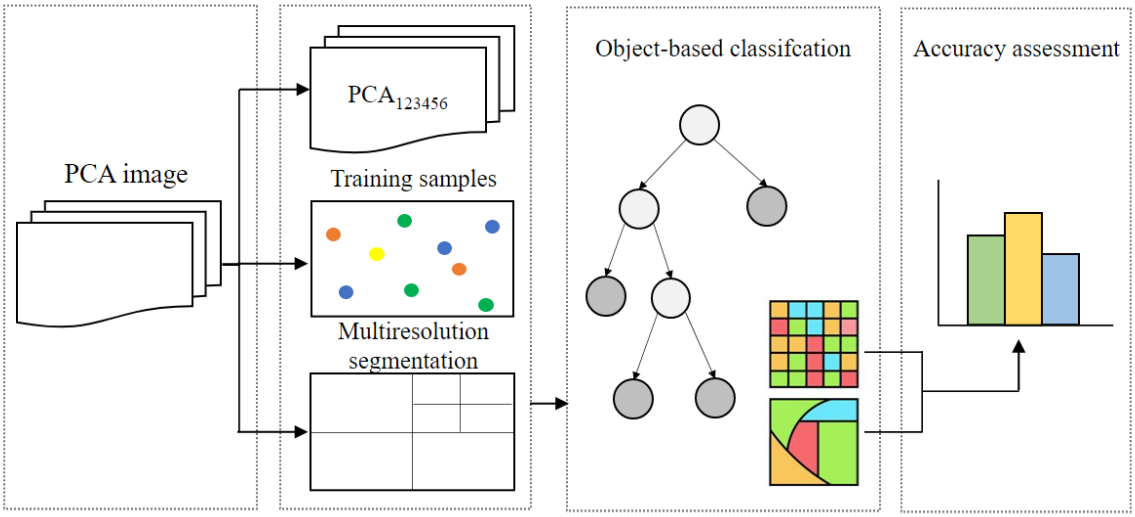

Figure 4. A general diagram of the classification scheme.

In order to evaluate the performance of the object-based classification in classifying the selected PC features, the accuracy assessments have been performed based on the sample pixels defined by analyst's experience and local knowledge, and the results are shown in Table 2. As seen from the Table 2, the PC236 combination demonstrated the highest accuracy (overall accuracy=83.39%, and Kappa coefficient=0.776), while PCA123 combination showed the lowest accuracy (overall accuracy=66.93%, and Kappa coefficient=0.552). The second highest accuracy was obtained by the PCA123456 combination (overall accuracy=80.02%, and Kappa coefficient=0.722). The performance of the PCA2345 combination was insufficient (overall accuracy=77.08%, and Kappa coefficient=0.682), but it was higher than the result of the first three PCs. As seen, the combination that includes PC1 could demonstrate a deficient result, even it contains the largest amount of the overall variance.

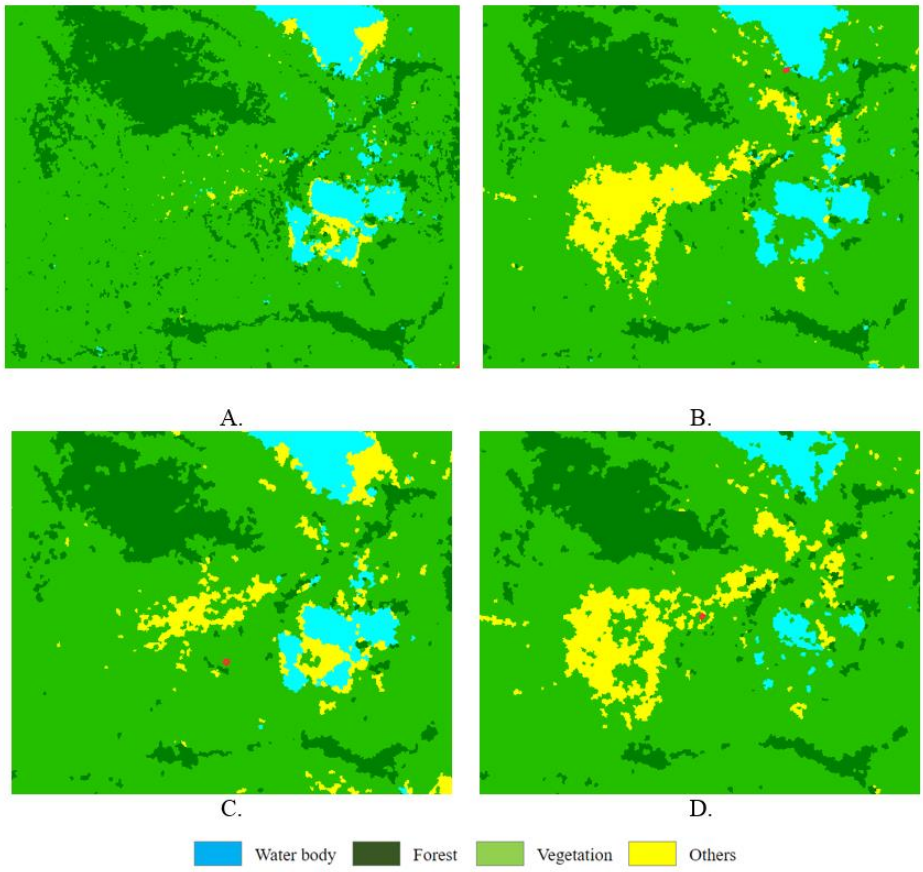

Figure 5. The classification results of A) PCA123, B) PCA236, C) PCA2345, and D) PCA123456.

Table 2. Classification accuracies.

Feature combination	Overall accuracy %	Kappa coefficient
PCA123	66.93	0.552
PCA236	83.39	0.776
PCA2345	77.08	0.682
PCA123456	80.02	0.722

5. CONCLUSION

The aim of this research was to evaluate the features derived from the PCA for an efficient land cover discrimination. For this purpose, Sentinel-1 microwave data and Sentinel-2 optical images, and object-based classification techniques were applied. The test site was found in the Erdenet area situated in northern part of Mongolia. For the classification of land cover types, four different combinations of the PCs such as PC123, PC236, PC2345, and PC123456 were chosen. The inspection of the PCs indicated, the PC1 that comprised the largest overall variance contained insufficient information related to the existing classes. Before applying the object-based method, a multi-resolution segmentation was applied to the selected features. The results of the classification were compared in terms of separation of the available classes. Among the selected PC combinations, the highest overall classification accuracy was achieved in the PC236 combination, while the lowest accuracy was obtained in the PC236 combination. Overall, the study showed that in the selected test site the PCs containing a minor amount of variance could still have useful information for land cover analysis.

REFERENCES

Amarsaikhan, D. and Saandar, M., 2011. Chapter 8 - Fusion of Multisource Images for Update of Urban GIS in "IMAGE FUSION AND ITS APPLICATIONS" BOOK published by InTECH Open Access Publisher, pp.127-152.

Amarsaikhan, D. and Ganchuluun, N., 2015. Chapter 4 –"Fusion and Classification of Multisource Images for Update of Forest GIS" in "IMAGE FUSION: PRINCIPLES, TECHNOLOGY AND APPLICATIONS", Nova Science Publishers, New York, USA, pp.83-121.

Comber, A.J., Harris, P. and Tsutsumida, N., 2016. Improving land cover classification using input variables derived from a geographically weighted principal components analysis. ISPRS Journal of Photogrammetry and Remote Sensing, 119. pp.347-360.

Datta, U., 2021. Multimodal change monitoring using multitemporal satellite images. Image and Signal Processing for Remote Sensing XXVII.

Drusch, M., Del Bello, U., Carlier, S., Colin, O., Fernandez, V., Gascon, F., Hoersch, B., Isola, C., Laberinti, P., Martimort, P., Meygret, A., Spoto, F., Sy, O., Marchese, F. & Bargellini, P., 2012. Sentinel-2: ESA's Optical High-Resolution Mission for GMES Operational Services. Remote Sensing of Environment, 120, pp.25-36.

Erdenet city, Retrieved Nov 1, 2021. Available at https://www.toursmongolia.com/destinations/erdenet-city.

Fang, F., Li, F., Zhang, G. and Shen, C., 2013. A variational method for multisource remote-sensing image fusion. International Journal of Remote Sensing, Vol. 34(7), pp.2470–2486.

Grenzdorffer, G.J., 2005. Land use change in Rostock, Germany since the reunification-a combined approach with satellite data and high-resolution aerial images, Proceedings of the ISPRS WG VII/ 1'Human Settlements and Impact Analysis'-3rd International Symposium Remote Sensing and Data Fusion over Urban Areas (Urban 2005) and 5th International Symposium Remote Sensing of Urban Areas (URS 2005), 14–16 March 2005, Tempe, Arizona.

Gupta, R., Tiwari, R., Saini, V. & Srivastava, N., 2013. A Simplified Approach for Interpreting Principal Component Images. Advances in Remote Sensing, 2(2), pp.111-119.

Haruna, A.A., 2019. Classification accuracy and trend assessments of land cover- land use changes from principal components of land satellite images. International Journal of Remote Sensing, 40(4), pp.1275-1300.

He, W. & Yokoya, N., 2018. Multi-Temporal Sentinel-1 and -2 Data Fusion for Optical Image Simulation. International Journal of Geo-Information.

Liu, D. and Xia, F., 2010. Assessing object-based classification: advantages and limitations. Remote Sens Lett. 1(4):187–194.

Munkh-Erdene, A., Amarsaikhan, D., Odontuya, G., Enkhjargal, D., E.Jargaldalai, 2021. Feature extraction approach in hyperspectral data, Advances in Engineering Research, Vol.206, Proceedings of the ESTIC 2021, Atlantis Press-Springer Nature, pp.102-108.

Neetu, N. and Ray, S. S., 2020. "Evaluation of different approaches to the fusion of Sentinel −1 SAR data and resources at 2 LISS III optical data for use in crop classification." Remote Sensing Letters 11 (12): 1157–1166

Nyamjargal, E., Amarsaikhan*, D., Munkh-Erdene, A., Battsengel, V., Bolorchuluun, Ch., 2019, Object-based classification of mixed forest types in Mongolia, Geocarto International, Vol.35, No.14, pp.1615-1626.

Quang, N. H., Tuan, V. A., Hao, N. T. P., Hang, L. T. T., Hung, N. M., Anh, V. L., Phuong, L. T. M., & Carrie, R., 2019. Synthetic aperture radar and optical remote sensing image fusion for flood monitoring in the Vietnam lower mekong basin: A prototype application for the Vietnam open data cube. European Journal of Remote Sensing, 52(1), 599–612.

Sritarapipat, T., Kasetkasem, T. and Rakwatin, P., 2014. Fusion and registration of THEOS multispectral and panchromatic images. International Journal of Remote Sensing, Vol.35(13), pp.5120-5147.

Wang, Q. & Atkinson, P.M., 2018. Spatio-temporal fusion for daily Sentinel-2 images. Remote Sensing of Environment, 204, pp. 31-42.

Weih, R.C. and Riggan, N.D., 2012. Object-based classification vs. pixel-based classification: comparative importance of multi-resolution imagery, The International Archives of Photogrammetry, Remote Sensing and Spatial Information Sciences, Vol. XXXVIII-4/C7.

Zhang, X., Du, S. & Wang, Q., 2018. Integrating bottom-up classification and top-down feedback for improving urban land-cover and functional-zone mapping. Remote Sensing of Environment, 212, pp. 231–248.